Aust. J. Phys., 1985, **38**, 337–51

A Neutron Spectrometer with a Two-dimensional Detector for Time-resolved Studies*

B. P. Schoenborn,[A] *A. M. Saxena,*[A] *M. Stamm,*[A,B] *G. Dimmler*[A] *and V. Radeka*[A]

[A] Brookhaven National Laboratory, Upton, NY 11973, U.S.A.
[B] On leave of absence from IFF/KFA, Postfach 1913, 5170 Jülich, Federal Republic of Germany.

Abstract

An intermediate resolution neutron spectrometer for collecting diffraction data with the range $Q = 0{\cdot}01$–$3{\cdot}0$ Å has been built for analysing the structural organization of membranes, polymers and other molecular aggregates. This spectrometer has a position-sensitive detector with a capability for time-resolved data collection which may be used to study conformational changes in dynamical systems. A double multilayer monochromator assembly is used to monochromate neutrons. Operating wavelengths of the spectrometer will be from 2 to 5 Å, and the wavelength bandwidth ($\Delta\lambda/\lambda$) can be adjusted within the 1%–8% range.

1. Introduction

Developments in instrumentation during the last decade have improved the capabilities of neutron spectrometers and made it possible to perform experiments of greater sophistication. These developments include (*a*) area detectors with a resolution of about 1 mm and an active area of up to 100×100 cm^2, which allow data collection over a large range of scattering angles without the necessity of moving the detector (Alberi *et al.* 1975; Allemende *et al.* 1975); (*b*) thin-film multilayer monochromators with very high reflectivities (Schoenborn *et al.* 1974; Saxena and Schoenborn 1977; Saxena and Majkrzak 1982); (*c*) neutron guides, either made of multilayer supermirrors or coated with ^{58}Ni, which can decrease the losses in transporting neutrons (Ebisawa *et al.* 1979; Scharpf 1982); (*d*) various crystal and mirror focusing devices for increasing the flux of neutrons at the sample (Saxena and Majkrzak 1984; Pynn 1984); and (*e*) use of array processors for fast handling of data from the detector. Some of these features have been incorporated in a neutron spectrometer which is being built for the H3B station of the High Flux Beam Reactor at Brookhaven National Laboratory. This spectrometer has a unique combination of features including a high resolution area detector, adjustable wavelength bandwidth, and capability for time-resolved data collection. It is designed to be used as an intermediate resolution spectrometer operating within the range $Q = 0{\cdot}01$–3 Å^{-1}, where Q is the modulus of the scattering vector $4\pi \sin\theta/\lambda$.

The monochromator assembly and the spectrometer are described in Sections 2 and 3. The area detectors developed at Brookhaven are discussed in Section 4, and

* Dedicated to Dr A. McL. Mathieson on the occasion of his 65th birthday.

0004-9506/85/030337$02.00

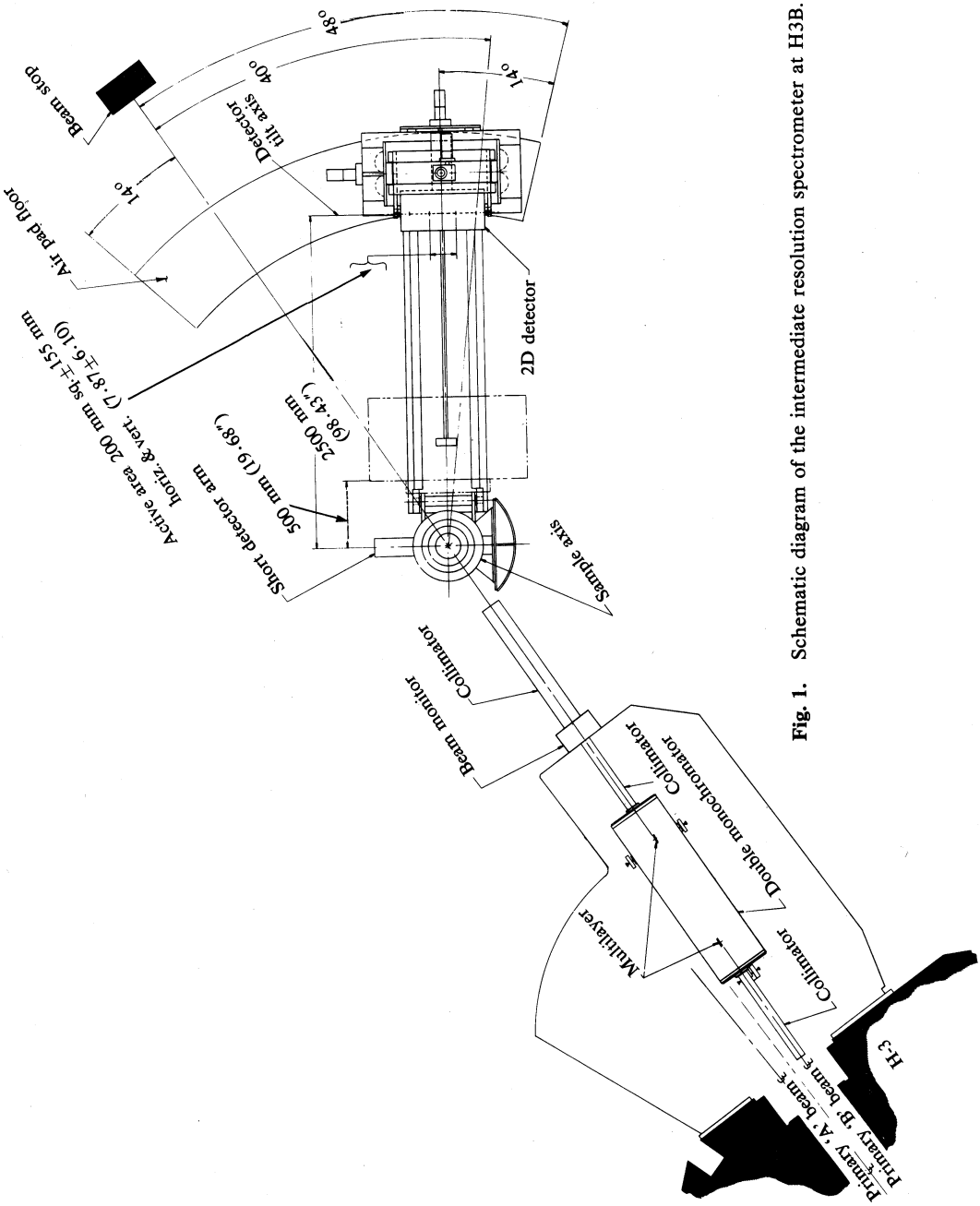

Fig. 1. Schematic diagram of the intermediate resolution spectrometer at H3B.

details of the time-slicing method for collecting data on rapidly changing systems are given in Section 5. Some of the structures that may be studied on this spectrometer are described in Section 6.

2. Monochromator

A schematic diagram of the H3B station is shown in Fig. 1. The neutron beam is first collimated by a steel collimator with a cross section of 1 cm (horiz.) by 2 cm (vert.). Monochromatization is achieved by reflecting the beam from two parallel multilayer monochromators. Multilayer monochromators of different combinations of materials are made by sputtering. A reflectivity of 95% can be obtained with Ni–Ti multilayers having a d spacing of 65 Å or more. Attempts are being made to decrease the minimum d spacing to 50 Å. An evacuated chamber containing monochromators and translation and rotation stages is located inside a shield made of steel, borated polyurethane and lead. The first multilayer is centred on the collimator axis, and is rotated to the appropriate angle to select the desired wavelength. The second multilayer can be rotated about a vertical axis and translated parallel to the incident beam with the help of a leadscrew to produce a final monochromatized beam which is always parallel to the incident beam and is displaced from it by 4 cm. Since the d spacing of a multilayer is about 55 Å, the scattering angle is only within the range 1°–4°, and the multilayers have to be rotated within this region.

A neutron beam reflected by a multilayer has a large wavelength bandwidth because of the small values of the scattering angles. Typical values of $\Delta\lambda/\lambda$ are from 7 to 10%. Although a large value of $\Delta\lambda/\lambda$ is desirable for low resolution studies because of the enhanced value of neutron flux, a smaller value of $\Delta\lambda/\lambda$ is required for higher resolution studies. This is achieved by a small rotation of the second multilayer from strict parallelism. The monochromator assembly is designed to work in the wavelength range 2·0–5·0 Å with values of $\Delta\lambda/\lambda$ between 1% and 8%.

Table 1. Characteristics of the H3B spectrometer

Wavelength	2·2–5·0 Å
Wavelength bandwidth ($\Delta\lambda/\lambda$)	0·01–0·08
Beam dimensions	1·0 cm (H)×2·0 cm (V)
Position-sensitive detector:	
Detector area	20×20 cm
Data array	512×256
Resolution	1·3 mm (H), 2·5 mm (V)
Distance from sample	50–250 cm
Angular scanning range	−5·0°–40·0°
Auxiliary detector:	
Distance from sample	30 cm
Angular scanning range	−5·0°–100·0°

3. Spectrometer and Computer System

The characteristics of the spectrometer are listed in Table 1. The spectrometer (built by Franke and Heydrich Precision Instruments, Federal Republic of Germany) consists of two separate units joined by a coupling arm. Each unit can be moved with low friction air pads. The sample table contains a rotational module for setting the sample angle. It has provisions for mounting a temperature- and humidity-controlled sample chamber and a superconducting magnet. Extending from this table is an

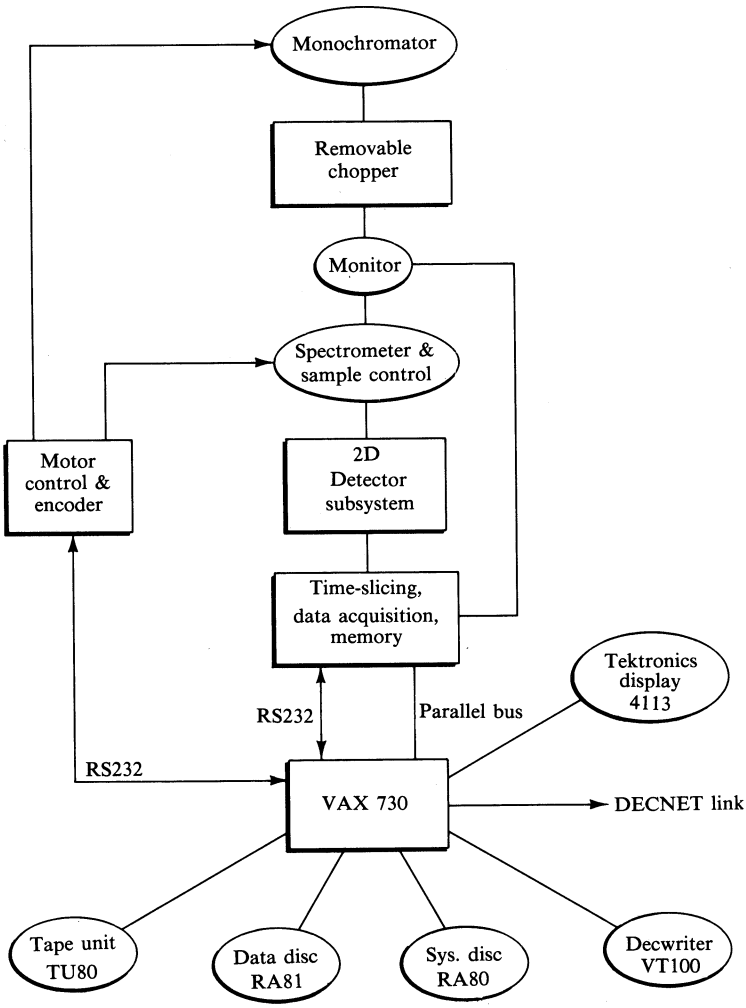

Fig. 2. Components of the spectrometer and experimental control.

auxiliary arm of length 30 cm which contains a Soller collimator and a ^{3}He detector for collecting high-angle data.

A 20×20 cm^2 area detector with its associated electronics is mounted on another unit which can also be moved with air pads. The scattering angle and the distance of the detector from the sample are changed by moving this unit with respect to the sample table. The detector can also be moved in the vertical direction and sideways (in a plane perpendicular to the beam) under computer control. The path between the detector and the sample is filled with helium to decrease air scattering. Because of the performance requirements of air pads, the entire floor area is flat within 0·005″.

Data from the detector are accumulated in a two-dimensional array having 256 channels in the horizontal direction and 128 channels in the vertical direction. Resolution of the detector is 1·3 and 2·5 mm in these two directions. Data flow and computer control are somewhat similar to those at the small-angle station (H9B)

on the cold source, as described by Schoenborn *et al.* (1983). Components of the spectrometer and experimental control are shown in Fig. 2. The motor control system moves and updates the positions of the monochromator and spectrometer axes. It accepts manual inputs as well as programmed commands from the data acquisition processor. Spectrometer settings are displayed locally and are available in the processor for on-line control. A VAX 11/730 computer system will be used for controlling the spectrometer, data acquisition and data analysis. Data arrays will be transferred to a 456 MB disc for temporary storage and analysis, and written on a magnetic tape for off-line analysis.

The use of a position-sensitive detector controlled by a computerized data acquisition system permits new approaches to data collection strategies. Instead of dealing with conventional scans, such as the ω–2θ scan, that provide integrated intensity as a function of a rotational parameter, a computer-linked counter can be used to produce a three-dimensional reflection profile, as described by Schoenborn (1983). By summing data for each ω over appropriate Y channels in the counter, one can also take a $(\Delta\omega, \Delta 2\theta)$ scan. Mathieson (1982) showed that this scan has the advantage of allowing a more precise specification of background, hence bypassing the problem of variable truncation, and therefore leads to improved accuracy in determining structure factors. This is all the more important for biological samples because of the large disorder in such samples and the higher background emanating from the hydrogen atoms in their structures. Software to perform background subtraction by this method has been installed in the VAX 11/730. Results of on-line analyses are displayed on a Tektronix 4113 terminal.

Dynamic processes and conformational changes in membranes or molecular aggregates under the influence of external stimuli can be studied by the time-slicing processor built into the data acquisition system. At the beginning of each time slice, the processor sets a map register defining the base address memory where data for the current time slice will be stored. Associated hardware then controls gating of the detector and auxiliary scalars. The processor will also be responsible for timing the ouput pulses and excitation voltages in accordance with the time-slice parameter list. The minimum switching time in the time-slice mode will be 200 ns. The time-resolved data collection subsystem developed for this spectrometer will also be used for structural studies at the National Synchrotron Light Source.

4. Two-dimensional Thermal Neutron Detector

(a) General

Two-dimensional position-sensitive detectors are being used increasingly in neutron diffraction experiments for the determination of molecular and crystal structures. These detectors are used within the wavelength range 1–8 Å. A useful position-sensitive detector should satisfy the following requirements: (1) high detection efficiency for neutrons and low efficiency for γ rays, (2) uniformity of efficiency over the entire area of the detector, (3) high positional resolution at counting rates up to 10^5 neutrons s^{-1}, (4) small scattering in the entrance window, and (5) stable operation over long periods of time.

The neutron detectors developed by us are gas proportional counters based on the charged particles from the reaction

$$^3\mathrm{He} + \mathrm{n} = {}^3\mathrm{H} + \mathrm{p} + 0{\cdot}764\ \mathrm{MeV}.$$

The reaction products (proton 573 keV and triton 191 keV) are emitted isotropically in opposite directions. Because of the large difference in the energies and ranges of the proton and the triton, the ionization centroid is displaced from the interaction point. The positional resolution limit is thus determined by the stopping power of the gas for the charged particles and the electronic noise in the position readout. A study of different gases has led to the use of a ^3He–C_3H_8 mixture, which has a high detection efficiency for neutrons, a high stopping power for protons and tritons, and a low cross section for γ rays.

A very sensitive position readout method has also been developed (Radeka and Boie 1980; Boie and Radeka 1980; Boie *et al.* 1982) which can detect an avalanche charge of less than one-tenth of a pC as compared with 1 pC in the conventional readout methods. This readout requires a gas gain of only 20–30, where the adverse effects of charge multiplication and space charge are negligible.

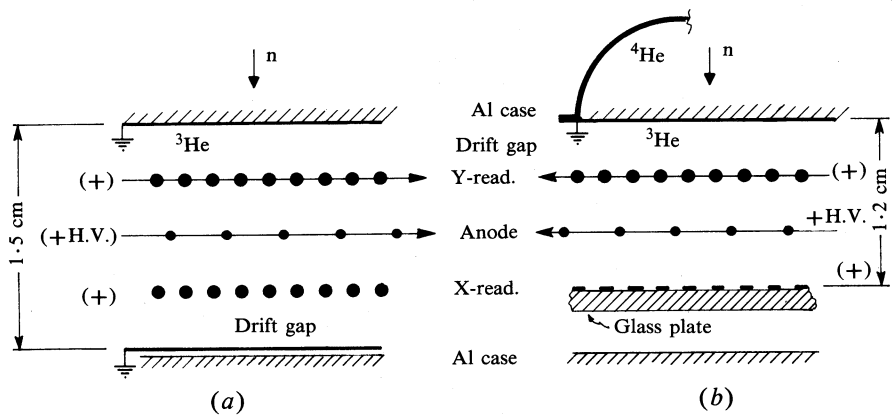

Fig. 3. Electrode configurations: (*a*) 20×20 cm^2 type detector and (*b*) 50×50 cm^2 detector with pressure containing dome. Arrows indicate the direction of anode and Y-readout wires, and circles indicate the relative spacing of wires.

(b) Electrode Geometry and Detector Configuration

The detector consists of an aluminum pressure vessel containing an electrode structure, an external closed-system circulating gas purifier, and preamplifiers that must be positioned close to the electrodes. The arrangement of electrodes is somewhat different for a 50×50 cm^2 detector than for a 20×20 cm^2 detector. Fig. 3*a* shows the symmetrical arrangement for the smaller detectors. The electrodes consist of two wire grid planes for position readout of induced charges, centred between the anode and each cathode. The readout grids are oriented such that one is parallel (grid Y) and the other is perpendicular (grid X) to the anode wires.

The asymmetric electrode arrangement of Fig. 3*b* is used for a detector area of 50×50 cm^2. A readout cathode of metal strips (X-axis) on a glass plate is substituted for one of the wire grids. A flat entrance window, 8–9 mm thick, is used for all the detectors but, for the larger detectors, it is further surrounded by a spherical dome filled with ^4He at the same pressure as the gas mixture inside the detector.

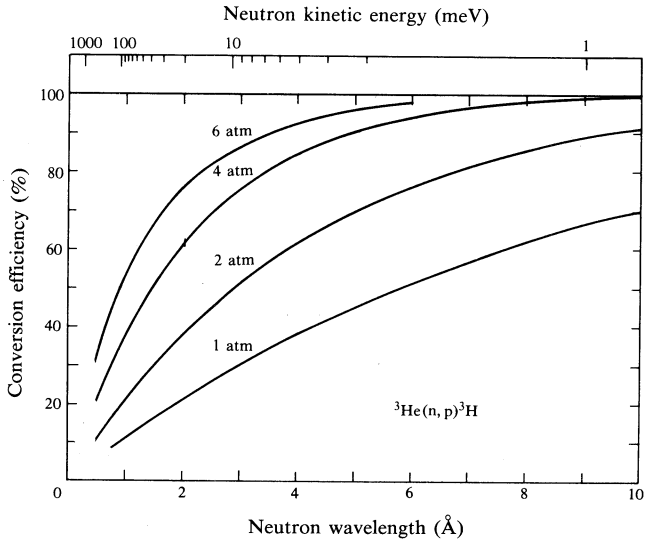

Fig. 4. Neutron conversion efficiency of ^{3}He against neutron wavelength at various pressures for an active thickness of 1·5 cm. (1 atm ≡ $1{\cdot}01\times10^5$ Pa.)

(c) Choice of Gas Mixture

Fig. 4 shows the conversion efficiency as a function of neutron wavelength for various pressures of ^{3}He. The thickness of the gas layer was assumed to be 1·5 cm for these calculations. This plot has been obtained from the known and measured neutron cross sections. The required partial pressure of ^{3}He in the gas mixture can be determined from curves of this type.

The range of protons emerging from the ^{3}He(n, p)^{3}H reaction is so broad in ^{3}He that a good position resolution cannot be obtained even at pressures of 5–6 atm. An additive with a higher stopping power is essential for good position resolution as well as for reducing wall effects on energy resolution. Since the detectors have to operate in a high photon background, the added gas should also have a low sensitivity for X rays and γ rays. The properties of different gases for neutron detectors were discussed in detail by Fischer *et al.* (1983). We have found that a mixture of ^{3}He at 6 atm and C_3H_8 at 2·5 atm has the desired characteristics. It is operated at an avalanche charge $Q_{sa} = 6\times10^5$ electrons, corresponding to a gas gain of about 20–30. This ensures a long chamber life with respect to deposit formation and negligible space charge effects at high counting rates.

(d) Position Readout

The principle of the high precision position-sensing method has been described by Radeka and Boie (1980) and is illustrated in Fig. 5. The readout grid wires are connected in groups of two or three, which are interconnected by a chain of resistors as shown. Low-input resistance amplifiers are connected to the resistance chain nodes at intervals determined by signal and noise considerations. When a neutron is detected,

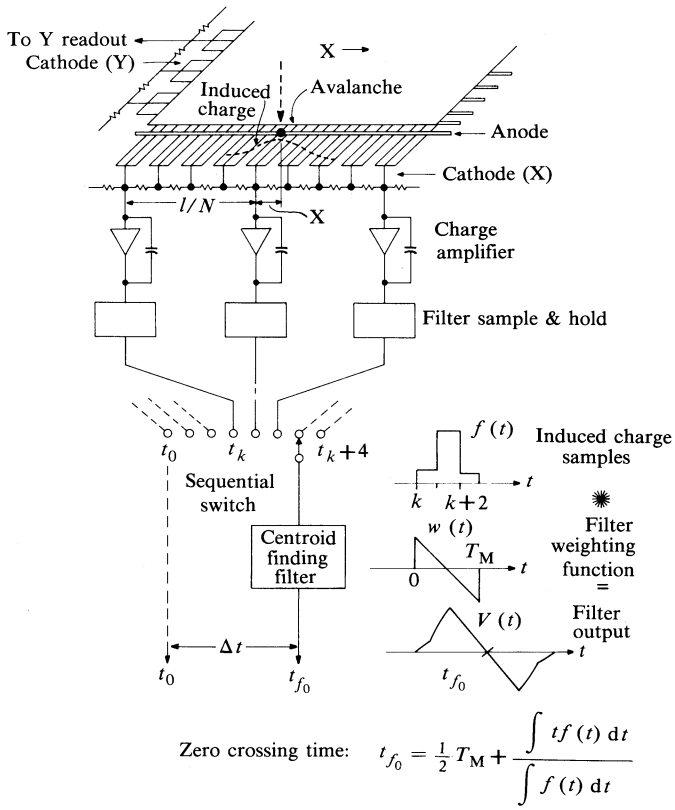

Fig. 5. Principle of the centroid-finding method by convolution. Preamplifier outputs from the subdivided resistance chain are switched sequentially into the centroid-finding filter. The zero crossing time t_{f0} is a continuous linear function of the position of the induced charge over the whole detector.

sample and hold circuits provide a stored measure of the induced-charge sharing on subdivision nodes. The centroid of the induced charge is then determined by convolution of the sequence of these samples with a linear centroid-finding filter. The zero crossing time of this filter is an exact linear measure of the position centroid, and the position scale is defined uniquely by the clock frequency of the sequential switch. The method achieves a high absolute position accuracy with small avalanche charge by virtue of a number of signal outputs from the detector, i.e. by the subdivision of the detector. Yet, this readout provides an output which is a continuous linear function of the position over the whole detector. The number of subdivisions is 16 for the smaller detector (20×20 cm^2) and 32 for the larger detector. Differential nonlinearity of the detector is found to be within ±2–3%.

Fig. 6 shows the measured position resolution on the 20×20 cm^2 detector for two values of the C_3H_8 pressure. These measurements were made with a 0·3 mm beam of 2·4 Å neutrons. The resolution measured at 2·5 atm of C_3H_8 and corrected for the beamwidth was 1·26 mm.

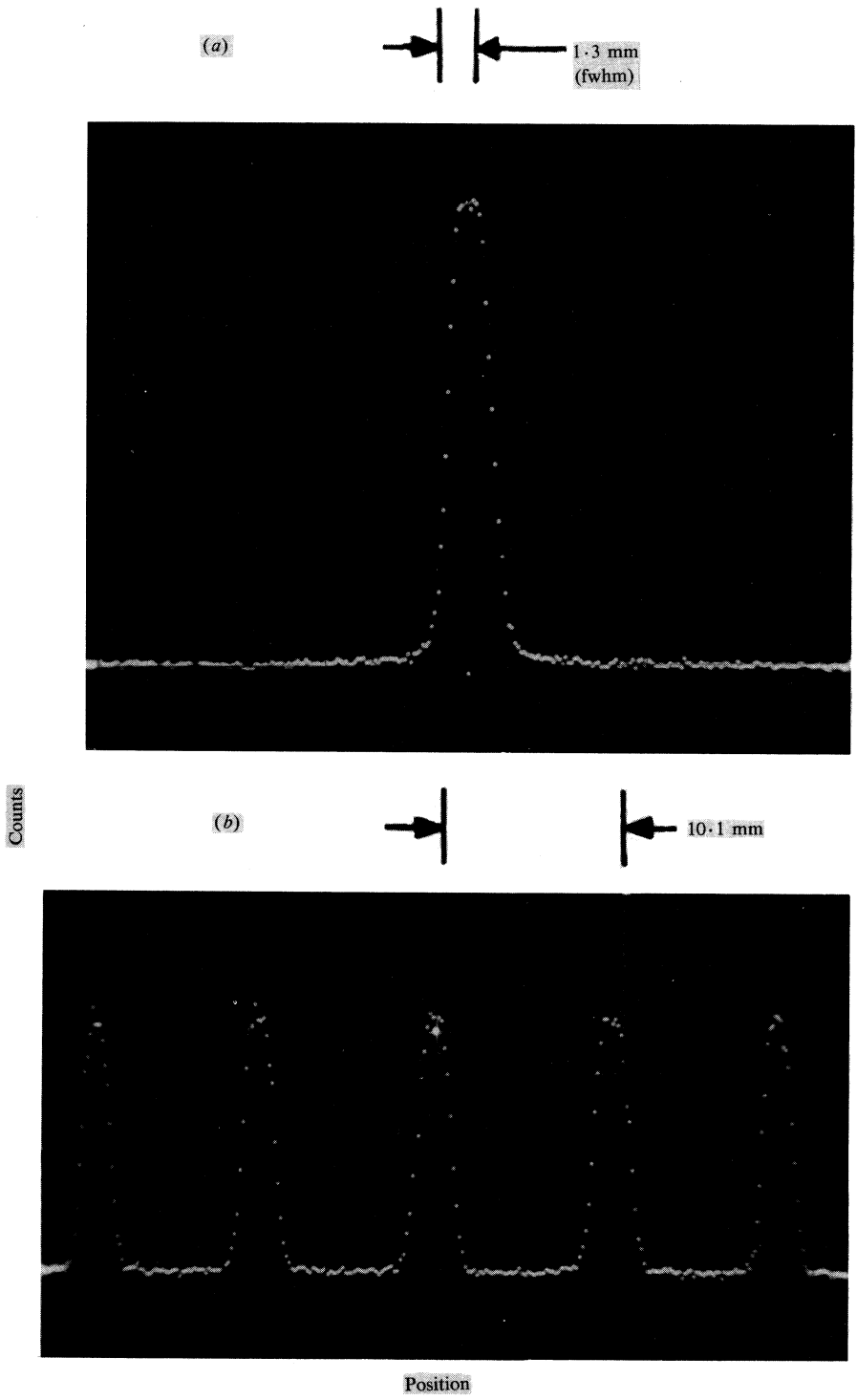

Fig. 6. Measured position resolution for 2·4 Å neutrons for the gas mixture $^3He + C_3H_8$ at (*a*) 2·5 atm and (*b*) 1·5 atm.

5. Time-resolved Data Collection

(a) General

The time-resolved data collection system allows for the connection of an array of position-sensitive area detectors each capable of up to 10^6 position elements. The total average event rate of all detectors can reach several times 10^5 events per second. A collection sequence may include several thousand slices with one time slice being as short as a few μs. Some of the advanced requirements met in this design are (i) a data memory independent of the computer memory in such a way that a high input data rate does not deteriorate the execution speed of the computer software; (ii) an address space of 2^{28} bytes, allowing for a large data memory not limited by addressing considerations; and (iii) a data memory directly addressable concurrently by several processors and input data streams via a cycle-stealing method. The significant features of the system are reviewed below; a more detailed description is given by Dimmler (1985).

(b) Data Flow

Initially, the device will have three channels. At any given time, the path from a given detector is connected to one slice of the appropriate data array in the memory. The size of one slice is determined by the number of X elements times the number of Y elements of the detectors. A data array for one detector consists of the number of slices necessary in a given experiment. The data paths between the various channels and data arrays are synchronously switched by a timing control subsystem as described below.

(c) Detector Interface

A detector delivers four signals to an assigned channel of the system: (1) a 64·0 MHz clock, (2) a BUSY signal level, (3) an X-GATE level, and (4) a Y-GATE level. The gate level widths are proportional to the values of the X and the Y positions of a detected event. For a 20 cm detector with 256 positions along each of the two axes, a time of ≈ 5 μs is necessary to decode the event position.

(d) Outline of System

As shown in Fig. 7, the four signals from each detector are accepted by a channel of the data input module (one module holds three channels). The data input module counts the clock pulses, which are bracketed by the X- and Y-GATE levels. When the BUSY level drops, the contents of the two counters, which now represent the position information of an event, are deposited into a 64-word first-in-first-out (FIFO) queue. Each channel requires one such queue. The FIFO queue is necessary to convert the random arrival rate of the events into a periodic rate suitable for event processing.

The base address of the slice is also, at this instant, recorded into the queue and becomes part of the event descriptor, which consists of 12 bits of X position, 12 bits of Y position, and 18 bits of base address. The strategy of queuing the base address with each event eliminates the undesirable dead time that often occurs with other designs during the switching to the next slice. The address calculation control picks up events from the FIFO queue, applies a series of validity tests, calculates the absolute memory address, and performs a direct-memory-increment function into the addressed location.

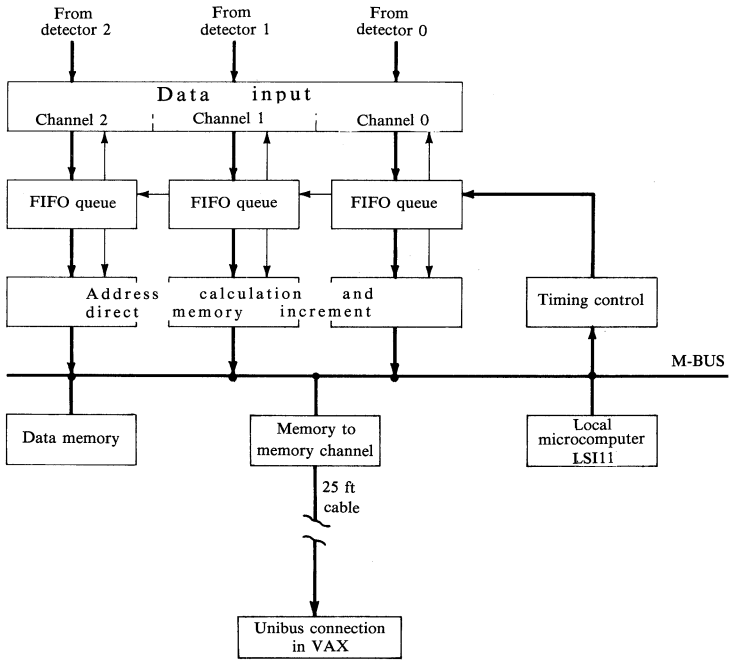

Fig. 7. Block diagram of the three-channel system.

Validity Tests. Four registers, which can be set by the host computer, contain the four corners of a window of interest within the two-dimensional address space of the time-slice memory. Events falling outside the window will be discarded at this point, where very little processing time has been used. This feature increases the effective maximum rate by eliminating the counting of possible high-rate background outside the window of interest.

Address Calculation and Direct Memory Increment. The range of the X-axis, which had been set by software at setup time, is multiplied in a 12×12 bit multiplier by the Y position of the event. The X position is added, and the content of the slice offset register is merged; this results in a 28-bit physical memory address. The arithmetic calculations take approximately 150 ns each, using high-speed VLSI chips (available from TRW and others). The content of the addressed 16-bit wide memory is then incremented by one bit, using two memory cycles of 600 ns each.

(e) Timing Control

The purpose of this segment is to control the timing sequence of a complete run after the system has been set up by the host computer. The resolution of the basic clock in the timing control can be set between 62·5 ns and 4·096 ms per step, where 1 μs per step is typical and is assumed in the subsequent discussion. Fig. 8 shows the essential parts of the timing sequence. Once the sequence is enabled by the host computer, a run can be started by any one of several possible conditions such as an external pulse, a host computer command, or the end of a pause after the previous

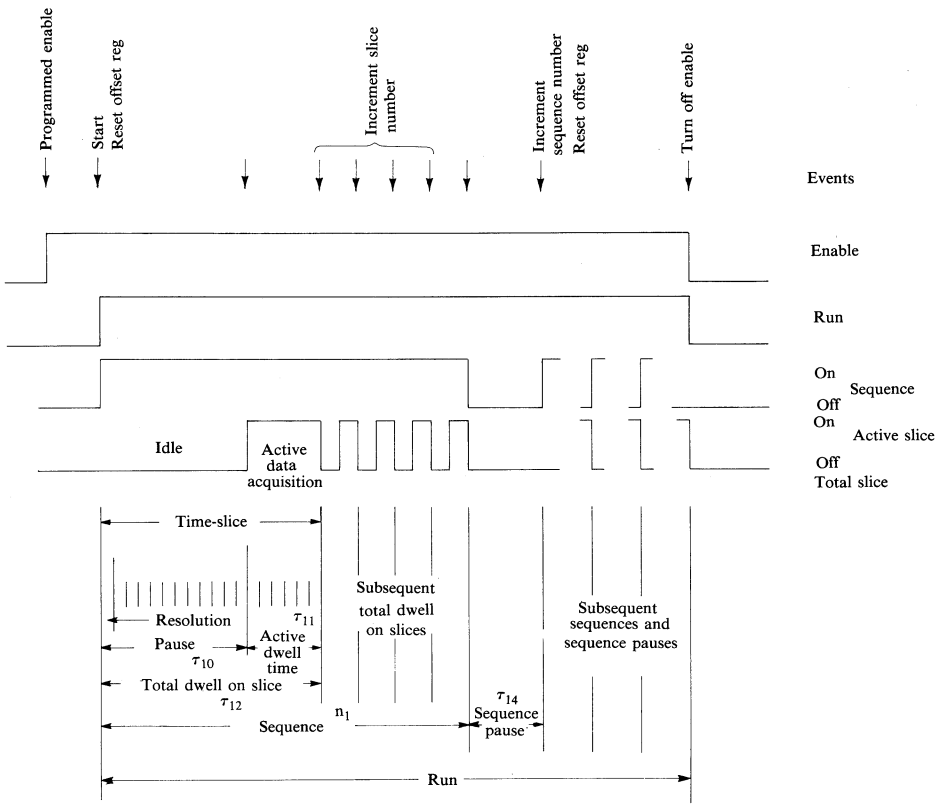

Fig. 8. Timing sequence for the time-slice unit.

sequence, as explained below. If several conditions are enabled, only the first one will start the sequence and the subsequent ones will be discarded. A time slice, which may have a maximum length of 4295 s at a 1 μs clock resolution, has two segments: (1) a pause during which the data acquisition channels are closed, and (2) an active dwell time when the channels accept and process events. The ratio between the segments is determined at the setup time. The timing control will handle up to 65 536 slices. The previously mentioned pause between two sequences may be set between 1 μs and 4295 s. At the start of a new sequence, the appropriate base address is picked up from a table, which had been filled at setup time. This method permits saving of memory by overlapping time slices in those segments of the sequence where a high time resolution is not necessary. These segments are usually found at the beginning and at the end of the sequence. A sequence may be repeated up to 65 536 times without intervention by the host computer.

(f) Connection to Host Computer

A memory-to-memory channel, as shown in Fig. 7, allows for block transfers between the data memory and the main memory of the host computer, which is a VAX 11/730. A transfer takes place at the maximum speed allowed by the host computer.

6. Uses of the Spectrometer

(a) Biological Samples

Since this is an intermediate resolution spectrometer, it is best suited for structural studies involving membranes, small molecules and molecular aggregates. The amount of disorder in biological membranes is often very large, limiting the resolution to which the structure can be analysed. The same is true for some of the model membranes. In these cases a high neutron flux is very useful to determine the background-subtracted intensities of reflections, and a relatively large value of $\Delta\lambda/\lambda$ can be accepted. A number of studies involve the insertion of small molecules such as alkanes, anaesthetics, drugs and peptides in lipid multilayers (see e.g. White *et al.* 1981). Information about gross structural changes occurring as a result of these insertions can still be obtained from low resolution studies. However, in well ordered systems, neutron diffraction combined with selective deuteration of molecules can give precise information about the location of molecular components (see e.g. Büldt and Seelig 1980). A detailed study of this type can be conducted only when the wavelength bandwidth of the incident beam is of the order of 1%. Variable $\Delta\lambda/\lambda$ of this spectrometer can enable one to study lamellar systems under optimum conditions.

The capability of time-resolved data collection can be used to study the dynamic behaviour of systems under the influence of ligands or external stimuli. Examples of such structures are microtubule assembly (Bordas *et al.* 1983), muscle contraction and relaxation (Faruqi 1983) and Ca^{2+}–ATPase of isolated sarcoplasmic reticulum (Blasie *et al.* 1985). As this technique becomes established, it is likely to find applications in many other fields as well.

(b) Synthetic Polymers

The field of synthetic polymers includes many areas where time-resolved neutron scattering data would be very helpful. The big advantage of neutron scattering over other methods comes from the fact that usually, even in the bulk, a very favourable contrast between chains can be achieved by deuteration of some of the molecules. Thus the conformation of a single unperturbed chain can be resolved; similarly, chain segments, specific phases or blocks, cross-linking points, or dopants can be marked by deuteration. This technique has proved to be very powerful in the case of static experiments, but kinetic investigations have been done only rarely, primarily because of lack of intensity for time scales smaller than approximately 1 min. One example of a real-time experiment in this time scale is an investigation of polymer interdiffusion (Stamm 1983) in which the small-angle scattering intensity of a polyethylene sandwich sample in the molten state was monitored as a function of time. Another experiment (Boue *et al.* 1982) has been performed with quenched-oriented polystyrene samples but, because of heating and quenching times, the time scale cannot be less than 10 s. Since during quenching the exact freezing temperature of the sample is generally not well known and, in some cases, structural changes take place (e.g. crystallization), a real-time experiment is much more favourable. Some suggested future time-resolved neutron experiments are (references indicate previous X-ray or light-scattering work):

(i) relaxation of chain segments in rubbery materials during stretching—a preliminary neutron scattering experiment by Rennie and Oberthür (1984) gave an indication of chain relaxation in the region of 0·1 s;

(ii) kinetics of crystallization and melting of semicrystalline polymers (Elsner *et al.* 1981);

(iii) development of stress-induced crystallization in some rubbers (Eisele 1979);

(iv) kinetics of spinoidal decomposition of polymer mixtures (Gilmer *et al.* 1982; Hashimoto *et al.* 1983; Snyder *et al.* 1983). Early stages are difficult to see by X-ray and light scattering;

(v) phase separation and crystallization of block copolymers (Hashimoto *et al.* 1981);

(vi) interdiffusion of polymers (Stamm 1983);

(vii) structural changes during the doping of electrically conducting polymers. Some experiments have been performed in the wide-angle region (Haesslin and Rieckel 1982; Stamm and Hocker 1983).

Most of these experiments might be performed in periodic repetition, some with a variable pause time used to restore the initial state and with the time-slice run started by a trigger signal.

Another feature of the new spectrometer is that it covers the intermediate region between small- and wide-angle scattering. This region is of particular interest in the detailed study of the chain conformation of semicrystalline polymers (Stamm *et al.* 1979; Stamm 1982; Fischer *et al.* 1984) as well as the orientation of chain segments in stretched polymers (Candau *et al.* 1982).

Acknowledgments

The principal collaborators for detector development have been J. Fischer, F. C. Merritt and L. C. Rogers. Contributions provided by R. Brown for engineering, E. Desmond for computer architecture, and V. Ramakrishnan and D. Schneider for software development are gratefully acknowledged. This work was supported by the Exxon Research and Engineering Company and the U.S. Deprtment of Energy.

References

Alberi, J., Fischer, F., Radeka, V., Rogers, L. C., and Schoenborn, B. P. (1975). *Nucl. Instrum. Methods* **127**, 507.

Allemende, R., Bourdel, J., Roudat, E., Convert, P., Ibel, K., Jacobe, J., Cotton, J. P., and Farnaux, B. (1975). *Nucl. Instrum. Methods* **126**, 29.

Blasie, J. K., Herbette, L., Pierce, D. H., Pascolini, D., Skita, V., and Scarpa, A. (1985). *Biophys. J.* (in press).

Boie, R. A., Fischer, J., Inagaki, Y., Merritt, F. C., Okuno, H., and Radeka, V. (1982). *Nucl. Instrum. Methods* **200**, 533.

Boie, R. A., and Radeka, V. (1980). *IEEE Trans. Nucl. Sci.* **NS-27**, 338.

Bordas, J., Mandelkow, E.-M., and Mandelkow, E. (1983). *J. Mol. Biol.* **164**, 89.

Boue, F., Nierlich, M., Jannink, G., and Bell, R. (1982). *J. Phys. (Paris)* **43**, 137.

Büldt, G., and Seelig, J. (1980). *Biochemistry* **19**, 6170.

Candau, S., Bastide, J., and Delsanti, M. (1982). *Adv. Polym. Sci.* **44**, 27.

Dimmler, D. G. (1985). Time-resolved data acquisition system for multiple high-resolution position-sensitive area detectors. Brookhaven Natl Lab. Rep. No. 51833.

Ebisawa, T., Achiwa, N., Yamada, S., Akiyoshi, T., and Okamoto, S. (1979). *J. Nucl. Sci. Tech.* **16**, 647.

Eisele, U. (1979). *Prog. Coll. Polym. Sci.* **66**, 59.

Elsner, G., Koch, M. H. J., Bordas, J., and Zachmann, H. G. (1981). *Macromol. Chem.* **182**, 1263.

Faruqi, A. R. (1983). *Nucl. Instrum. Methods* **217**, 19.

Fischer, E. W., Hahn, K., Kugler, J., Struth, U., Born, R., and Stamm, M. (1984). *J. Polym. Sci. Polym. Phys. Ed.* **22**, 1491.
Fischer, J., Radeka, V., and Boie, R. A. (1983). Proc. Workshop on Position-sensitive Detection of Thermal Neutrons (Eds Pierre Convert and J. Bruce Forsyth), p. 129 (Academic: New York).
Gilmer, J., Goldstein, N., and Stein, R. S. (1982). *J. Polym. Sci. Polym. Phys. Ed.* **20**, 2219.
Haesslin, H., and Rieckel, C. (1982). *Synth. Metals* **5**, 37.
Hashimoto, T., Kumaki, J., and Kawai, H. (1983). *Macromolecules* **16**, 641.
Hashimoto, T., Tasakahura, Y., and Kawai, H. (1981). *Macromolecules* **14**, 708.
Mathieson, A. McL. (1982). *Acta Crystallogr.* A **38**, 378.
Pynn, R. (1984). *Rev. Scient. Instrum.* **55**, 837.
Radeka, V., and Boie, R. A. (1980). *Nucl. Instrum. Meth.* **178**, 543.
Rennie, A. R., and Oberthür, R. C. (1984). *Rev. Phys. Appl.* **19**, 765.
Saxena, A. M., and Majkrzak, C. F. (1982). 'Neutron Scattering' (Ed. J. Faber), p. 193 (Am. Inst. Phys.: New York).
Saxena, A. M., and Majkrzak, C. F. (1984). 'Neutrons in Biology' (Ed. B. P. Schoenborn), p. 143 (Plenum: New York).
Saxena, A. M., and Schoenborn, B. P. (1977). *Acta Crystallogr.* A **33**, 805.
Scharpf, O. (1982). 'Neutron Scattering' (Ed. J. Faber), p. 182 (Am. Inst. Phys.: New York).
Schoenborn, B. P. (1983). *Acta Crystallogr.* A **39**, 315.
Schoenborn, B. P., Caspar, D. L. D., and Kammerer, O. F. (1974). *J. Appl. Crystallogr.* **7**, 508.
Schoenborn, B. P., Wise, D. S., and Schneider, D. K. (1983). *Trans. Am. Crystallogr. Assoc.* **19**, 69.
Snyder, H. J., Meakin, P., and Reich, S. (1983). *Macromolecules* **16**, 757.
Stamm, M. (1982). *J. Polym. Sci. Polym. Phys. Ed.* **20**, 235.
Stamm, M. (1983). *Am. Chem. Soc. Polym. Prepr.* **24**, 380.
Stamm, M., Fischer, E. W., and Dettenmaier, M. (1979). *Faraday Discuss. Chem. Soc.* **68**, 263.
Stamm, M., and Hocker, J. (1983). *J. Phys.* C3, **44**, 667.
White, S., King, G., and Cain, J. E. (1981). *Nature* **790**, 161.

Manuscript received 19 December 1984, accepted 29 March 1985